LAWRENCE
LIVERMORE
NATIONAL
LABORATORY

UCRL-JRNL-236557

# Direct Measurements of an increased threshold for stimulated Brillouin scattering with polarization smoothing in ignition hohlraum plasmas

D. Froula, L. Divol, R. L. Berger, R.A. London, N.B. Meezan, P. Neumayer, J. S. Ross, S. Stagnito, L. Suter, S. H. Glenzer

November 14, 2007

Physics Review Letters

## Disclaimer

# Direct measurements of an increased threshold for stimulated Brillouin scattering with polarization smoothing in ignition hohlraum plasmas

D. H. Froula,* L. Divol, R. L. Berger, R. A. London, N. B. Meezan, D. J. Strozzi, P. Neumayer, J. S. Ross, S. Stagnito,† L. J. Suter, and S. H. Glenzer
*L-399, Lawrence Livermore National Laboratory, P.O. Box 808, Livermore, CA 94551, USA*
(Dated: November 9, 2007)

We demonstrate a significant reduction of stimulated Brillouin scattering by polarization smoothing. The intensity threshold is measured to increase by a factor of $1.7 \pm 0.2$ when polarization smoothing is applied. The results were obtained in a high-temperature ($T_e \simeq 3$ keV) hohlraum plasma where filamentation is negligible in determining the backscatter threshold. These results are explained by an analytical model relevant to ICF plasma conditions that modifies the linear gain exponent to account for polarization smoothing.

PACS numbers: 52.25.Os, 52.35.Fp, 52.50.Jm
Keywords: laser plasma, laser beam propagation, polarization smoothing, SSD

Inertial confinement fusion (ICF) at megajoule laser facilities [1, 2] requires a high degree of uniformity in the laser focal spot intensity distribution to reduce laser-plasma instabilities in the indirect-drive approach [3] and hydrodynamic instabilities for directly driving fusion capsules [4]. The current indirect-drive approach to ICF requires that laser beams efficiently convert laser energy into soft x-rays after propagating through centimeter long, low-density, high-temperature plasmas.

The physics of creating the required radiation pressure within the ignition hohlraums may be dominated by the laser-plasma interactions in the plasma where laser backscattering, beam deflection, beam filamentation, and self focusing may occur when driving the intensity of the laser beam beyond their respective instability thresholds. The goal of present ignition designs is to choose a laser intensity that provides the required radiation temperature while backscatter instabilities remain below the threshold and remain energetically unimportant. We define the threshold for backscatter as the intensity ($I_{th}$) at which 5% of the incident power is backscattered from the hohlraum target.

To shape the laser focal spot and to smooth the inherent abberations produced by large high power glass lasers, continuous phase plates (CPP) [6] are used. These CPPs create a high contrast intensity pattern in the target plane with small-scale high-intensity structures (speckles). These speckles can play an important role in the dynamics of the laser-plasma interactions [7–11]. The high intensity contrast created by the CPP can instantaneously be reduced when applying polarization smoothing to the laser beam [12, 13].

Experiments in long-scale plasmas have shown the effect of polarization smoothing on the reduction of filamentation [14] and have demonstrated small reductions in backscatter [15–18]. These experiments were performed at intensities well above the threshold for backscatter and the main effect of polarization smoothing on the backscatter was inferred to be through the mitigation of ponderomotive filamentation. The effect of polarization smoothing was further investigated at lower electron temperatures ($T_e < 1$ keV) and in short scale-length plasmas where it was shown that polarization smoothing indeed strongly reduces thermal filamentation in speckles leading to a reduction in backscatter [19–21].

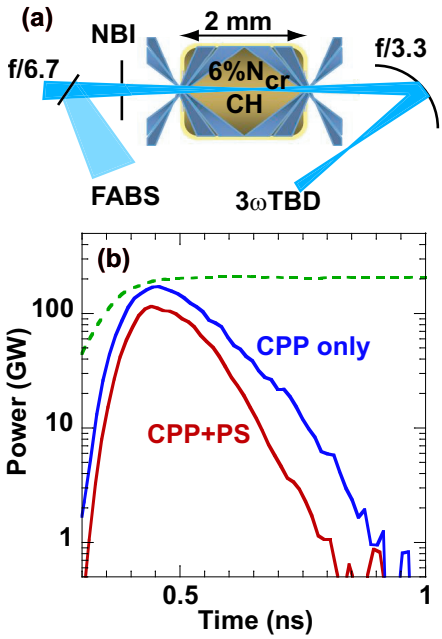


FIG. 1: (color) (a) A high power 351 nm interaction beam propagates along the axis of a 2-mm long hohlraum. The transmitted light is measured by the $3\omega$ TBD while the backscattered light is collected by a FABS and NBI. (b) The measured SBS power is shown to be low at all times when polarization smoothing (blue curve) is added to a CPP smoothed beam (red curve); an incident power of 200 GW is used (green dashed curve). The reflectivity peaks early in time as the interaction beam reaches maximum power and the plasma is cold ($T_e \sim 2$ keV); the backscatter decreases rapidly as the electron temperature increases [5].

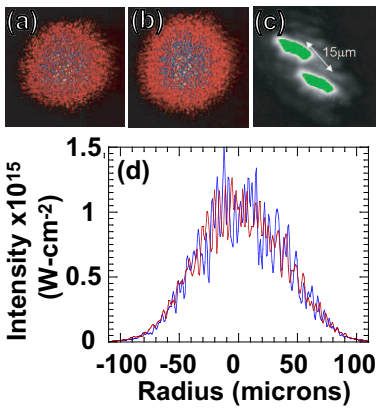


FIG. 2: (color) The far-field intensity distribution is simulated using the Omega laser beam abberations, the (a) measured CPP phase, and the (b) measured PS shift. (c) The polarization shift at the best vacuum focus was measured to be 15 microns. (d) The vacuum transverse intensity profile is compared with (red) and without polarization smoothing (blue) demonstrating an undetectable change in the average intensity when polarization smoothing is applied.

In this study, we present experiments that demonstrate, for the first time, the significant reduction of stimulated Brillouin scattering (SBS) by polarization smoothing in conditions with no filamentation. Figure 1 shows the experiment setup and the measured reduction of SBS when polarization smoothing is applied. We present measurements that show adding polarization smoothing increases the intensity threshold for SBS by a factor of $1.7\pm0.2$. For intensities less than $2\times10^{15}$ W-cm$^{-2}$, more than an order of magnitude reduction in the backscattered power is observed. The study is performed in a high temperature ($T_e \simeq 3$ keV) ICF relevant plasma where ponderomotive and thermal filamentation effects are measured to be negligible. An analytical model is presented that explains the effect of beam smoothing on the backscatter threshold.

A hohlraum target platform (Fig. 1a) for studying laser-plasma interactions in 2-mm long high-temperature plasmas has been developed by aligning an interaction beam down the axis of a gas-filled gold cylinder (hohlraum); this allows direct measurements of the laser beam propagation and transmission at ignition hohlraum plasma conditions [22]. The hohlraum is heated by thirty-three, 1-ns square pulsed, frequency tripled ($\lambda_o =$ 351 nm) laser beams (14.5 kJ) at the Omega Laser Facility [23]. The heater beams are smoothed by elliptical phase plates that project a $\sim$ 250 micron diameter intensity spot at the 800 micron diameter laser entrance holes.

The 1.6-mm diameter, 2-mm long hohlraum targets produce a uniform density plateau using 1 atm of gas fill consisting of 30% $CH_4$, and 70% $C_3H_8$ expressed as partial pressures. The plasma conditions along the interaction beam path ($T_e \simeq 3$ keV, $n_e \simeq 5\times10^{20}$ cm$^{-3}$) are comparable to the plasma conditions that the inner beam propagates through on current targets planned for ignition experiments on the National Ignition Facility [24]. Two-dimensional HYDRA [25] hydrodynamic simulations show a uniform 1.3-mm long plasma with a peak electron temperature of 3.5 keV. Previous studies have validated these plasma conditions using Thomson scattering [22] and provide confidence in the hydrodynamic parameters used as the initial conditions for laser-plasma interaction modeling.

Figure 2a shows the simulated far-field laser spot for the $3\omega$ interaction beam focused by a $f/6.7$ lens through a CPP. The simulated spot is generated using the Omega abberation model and the measured CPP near field phase. Figure 2d shows the intensity profile of the simulated laser spot averaged over 50 microns. The average on axis intensity at best focus for this beam is $I = 1.05\times\mathrm{P[GW]}\times10^{13}$ W-cm$^{-2}$, where P is the incident laser beam power ranging from 50 GW to 500 GW.

A new birefringent polarization smoothing crystal has been designed for these experiments that sufficiently separates the speckles in the far field without affecting the average spot size. After the laser beam propagates through this crystal, two beams separated by a small angle are created with equal intensity and orthogonal polarizations. The separation between the two beams was characterized to be 15 microns at best vacuum focus (Fig. 2c). When used with a CPP, this 15 micron separation at the focal plane is sufficient to decorrelate the two speckle patterns while having a minimal effect on the average intensity of the laser beam (Fig. 2d).

Light scattered from the interaction beam is measured using a full-aperture backscatter station (FABS), a near backscatter imager (NBI), and a $3\omega$ transmitted beam diagnostic ($3\omega$TBD) [26]. Light scattered back into the original beam cone is collected by the FABS; both stimulated Brillouin scattering (SBS) and stimulated Raman scattering (SRS) spectra and energies are independently measured. The NBI measures backscattered light outside the original beam cone that reflects from a plate surrounding the interaction beam. The plate is imaged onto two charge-coupled devices (CCDs) which time integrate the SBS and SRS signals. In this study, a new calibration technique was employed using a pulsed calibration system to deliver a known energy to the NBI scatter plate and the FABS calorimeters. The uncertainty in the measurements of the total SBS energy using this system is 5%. The $3\omega$TBD allows us to accurately measure the interaction beam power after propagating through the plasmas. In addition, the transmitted energy, spectrum, and beam spray are recorded. The system collects the forward scattered light within twice the original $f/6.7$ beam cone.

Figure 3 shows that the intensity threshold for a CPP smoothed laser beam is $I_{th} = 1.3\times10^{15}$ W-cm$^{-2}$. Adding

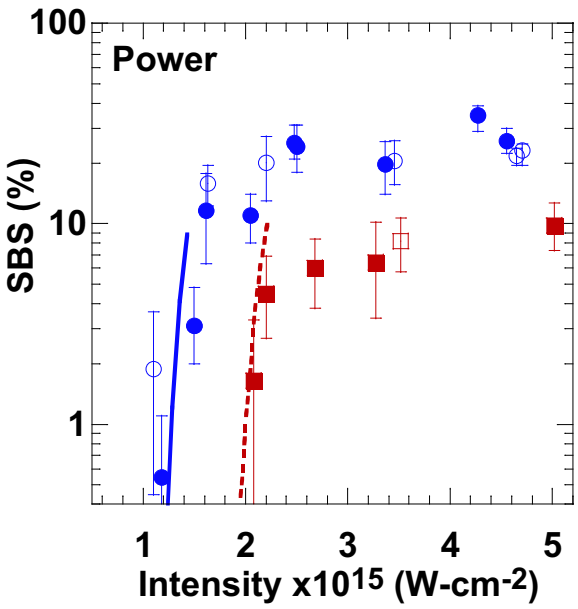


FIG. 3: (color) The measured instantaneous SBS reflectivity at 700 ps is plotted as a function of the interaction beam intensity; three laser smoothing conditions are shown: CPP (blue), PS (red), and 3Å SSD (open symbols). The calculated reflectivities using an analytical model reproduce the measured thresholds and the factor of 1.7 reduction in the SBS threshold when polarization smoothing is applied to a CCP smoothed laser beam. An analytical model (Eqs. 1 and 2) that calculates the thresholds is shown for the CPP only (solid blue curve) and when polarization smoothing is applied (dashed red curve).

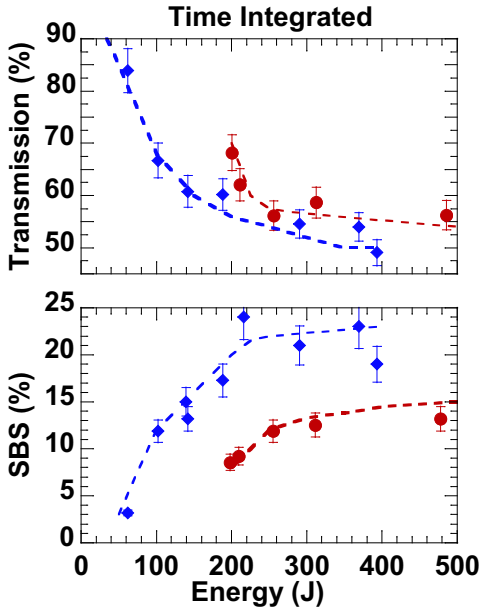


FIG. 4: (color) The time integrated transmission (top) and backscatter (bottom) are plotted as a function of interaction beam power. When polarization smoothing is applied (red circles), the transmission is increased and backscatter reduced consistent with reducing the laser power by a factor of two when polarization smoothing is not applied (blue diamonds).

polarization smoothing increases this threshold to $I_{th} = 2.2\times10^{15}$ W-cm$^{-2}$. This factor of 1.7±0.2 increase in the experimentally determined SBS threshold is consistent with modeling. Furthermore, polarization smoothing reduces the SBS reflected power by more than a factor of 10 for an incident intensity below $I = 2\times10^{15}$ W-cm$^{-2}$ and about a factor of 3 for incident intensities between $2\times10^{15}$ W-cm$^{-2} < I < 5\times10^{15}$ W-cm$^{-2}$, where the latter condition approaches the heavily driven regime where pump depletion becomes a factor. Adding 3Å of SSD to the bandwidth of the interaction beam has no measurable effect on SBS (Fig. 3). The SBS power is obtained by averaging the temporally resolved SBS reflectivity over 50 ps, 700 ps after the rise of the heater beam, prior to the shock wave produced by the ablation of the gold wall reaching the hohlraum axis, around t $\simeq$ 1.1ns. The error bars are given by the extreme reflectivities within the 50 ps time interval.

Figure 4 shows the total energy backscattered and transmitted through the plasma. For low backscatter conditions, more than 75% of the energy is transmitted through the plasma. For an incident laser energy of 200 J, polarization smoothing increases the total energy transmitted from 60% to 70% while the backscattered energy is reduced from 19% to 8%.

Figure 5 shows no measurable difference in beam spray when polarization smoothing is applied; as beam spray is a measure of filamentation, this is direct evidence that filamentation is not the main contribution to the measured effects of polarization smoothing on SBS. Furthermore, less than 5% of the the total SBS is measured outside of the FABS for incident interaction beam intensities less than $I < 3\times10^{15}$ W-cm$^{-2}$. These results are explained by the fact that the experiments remain below the thermal and ponderomotive filamentation thresholds by interacting with high electron temperature ($T_e \simeq 3$ keV) plasmas and by using moderate laser intensities.

The SBS intensity threshold determined using a detailed 1D model (DEPLETE [27]) predicts the threshold for SBS to be $2.2\times10^{15}$ W-cm$^{-2}$ which is higher than the measured threshold made with a CPP smoothed laser beam $1.3\times10^{15}$ W-cm$^{-2}$. DEPLETE uses the HYDRA simulation parameters and the average laser intensity on axis to calculate the laser and backscattered intensities, in steady state, along a 1D ray profile. It solves a set of scattered-wave coupled equations over a range of frequencies including realistic noise sources and pump depletion.

This measured enhancement of the SBS threshold is explained by a simple model that quantifies the effects of beam smoothing on the growth of SBS. In this model, we divide the plasma in to $n = L/L_{sp} = 19$ one-speckle-long slabs ($L_{sp} = 5f^2\lambda = 78\ \mu m$). By averaging the

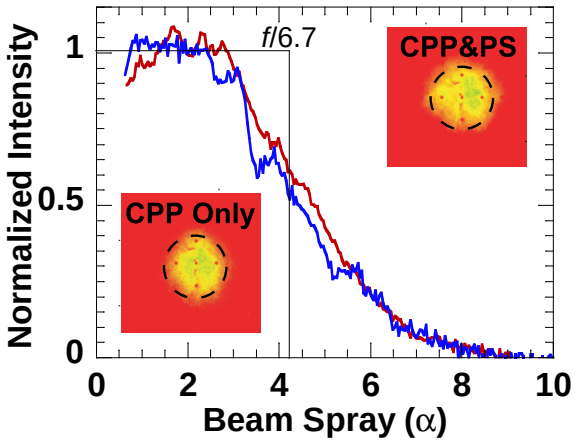


FIG. 5: (color) The intensity profile of the transmitted beam spray is plotted for an incident intensity of $2 \times 10^{15}$ W-cm$^{-2}$ and for two laser beam smoothing conditions: CPP only (blue), and CPP & PS (red). The near-field transmitted beam images are inset. The dashed circles represent a f/6.7 cone ($\alpha = 4.3^o$) around the center of the beam.

SBS growth over the intensity distribution for a laser beam model with a CPP, $P(I) = \exp(-I)$, the average gain exponent over one slab is $\langle G_{sp}^{CPP} \rangle \simeq G_{sp}(1+G_{sp}/2)$ provided the linear gain over one speckle is small ($G_{sp} \equiv G_{1D}/n << 1$) [8]. The gain over the entire plasma length (L=1.5 mm) is then given by adding the gain from each independent slab,

$$\langle G^{CPP} \rangle \simeq n \langle G_{sp}^{CPP} \rangle \simeq G_{1d}\left(1 + \frac{G_{sp}}{2}\right) \qquad (1)$$

From here it is evident that the effective gain is increased from the 1D value when the intensity distribution created by the CPP is included. At the measured threshold intensity ($I_{th}^{CPP} = 1.3 \times 10^{15}$ W-cm$^{-2}$), the 1D gain is $G_{1D} = 14.4$. This leads to a gain per speckle of $G_{sp} = 0.7$ and a correction to the 1D gain of $\langle G \rangle / G_{1d} = 1.4$. Using Eq. 1, the scattered reflectivity can be calculated by exponentiating the linear gain [$R \sim \epsilon \exp \langle G \rangle$] from an effective thermal noise determined by fitting the DEPLETE noise source calculations ($\epsilon = 10^{-11}$). The result agrees well with the experimental measurements (Fig. 3).

This model can be extended to include the effects of polarization smoothing. By splitting the power into two independent speckle patterns with orthogonal polarizations, the intensity distribution becomes $P(I) = 4I \exp(-2I)$. Further assuming that the polarizations are uncorrelated between successive slaps of speckles, the average gain exponent over the entire plasma length is obtained,

$$\langle G^{ps} \rangle \simeq -n \ln\left(\frac{1}{2} - \frac{1}{(4-2G_{sp})^2}\right) \simeq \frac{G_{1d}}{2}\left(1 + \frac{G_{sp}}{2}\right) \qquad (2)$$

This is a factor of 2 lower than Eq. 1, and the corresponding reflectivities agree well with the experiment (Fig. 3).

Note that while the decrease in the SBS threshold over the 1D result is due to the high beam contrast when a CPP smoothing is applied, the increase when PS is applied results from the mixing of the polarizations, not to a reduction of the beam contrast. This effect of PS applies to any high-temperature, long plasma where the gain per speckle remains much less than two, as is the case for most of the current ignition designs for NIF.

In summary, we have demonstrated a significant reduction in the backscattered power when polarization smoothing is applied and the plasma temperature exceeds $T_e > 2.5keV$. This reduction in backscatter is shown to increase the total transmission through a plasma for conditions that are comparable to those in current ICF target designs. A simple model, relevant to ICF plasma conditions, is presented that explains a direct effect on the SBS gain exponent, and consequently the threshold for when SBS becomes energetically important.

This work was supported by LDRD 06-ERD-056 and performed under the auspices of the U.S. Department of Energy by Lawrence Livermore National Laboratory under Contract DE-AC52-07NA27344.

* Electronic address: froula1@llnl.gov
† Laboratory for Laser Energetics, Rochester, NY

[1] E. Moses and E. Al., Fussion Sci. Tech. **47**, 314 (2005).
[2] C. Cavailler, Plasma Phys. Control. Fusion **47**, B389 (2005).
[3] J. D. Lindl et al., Phys. Plasmas **11**, 339 (2004).
[4] T. R. Boehly et al., J. Appl. Phys. **85**, 3444 (1999).
[5] D. H. Froula et al., Phys. Rev. Lett. **98**, 085001 (2007).
[6] S. Dixit et al., Opt. Lett. **21**, 1715 (1996).
[7] E. Lefebvre et al., Phys. Plasmas **5**, 2701 (1998).
[8] H. A. Rose and D. F. Dubois, Phys. Rev. Lett. **72**, 2883 (1994).
[9] D. S. Montgomery et al., Phys. Rev. Lett. **84**, 678 (2000).
[10] H. Baldis et al., Phys. Rev. Lett. **80**, 1900 (1998).
[11] V. T. Tikhonchuk et al., Phys. Plasmas **3**, 3777 (1996).
[12] K. Tsubakimoto et al., Opt. Commun. **91**, 9 (1992).
[13] D. H. Munro et al., Appl. Opt. **43**, 6639 (2004).
[14] S. H. Glenzer et al., Nature Physics **3**, 716 (2007).
[15] B. Macgowan et al., Phys. Plasmas **3**, 2029 (1996).
[16] D. S. Montgomery et al., Phys. Plasmas **3**, 1728 (1996).
[17] S. H. Glenzer et al., Phys. Plasmas **8**, 1692 (2001).
[18] J. D. Moody et al., Phys. Rev. Lett. **86**, 2810 (2001).
[19] J. Fuchs et al., Phys. Rev. Lett. **84**, 3089 (2000).
[20] S. Huller et al., Phys. Plasmas **5**, 3794 (1998).
[21] R. Berger et al., Phys. Plasmas **6**, 1043 (1999).
[22] D. Froula et al., Phys. Plasmas **13**, 052704 (2006).
[23] T. Boehly et al., Opt. Commun. **133**, 495 (1997).
[24] D. A. Callahan et al., Phys. Plasmas **13** (2006).
[25] M. M. Marinak et al., Phys. Plasmas **8**, 2275 (2001).
[26] D. H. Froula et al., Rev. Sci. Instrum. **77**, 10E507 (2006).
[27] D. J. Strozzi et al., To be published (2007).